Encapsulation of Magnetic and Fluorescent Nanoparticles in Emulsion Droplets

Swapan K. Mandal,[†] Nicolas Lequeux,[†] Benjamin Rotenberg,[†] Marc Tramier,[‡] Jacques Fattaccioli,[†] Jerome Bibette,[†] and Benoit Dubertret*[,§]

Laboratoire colloïdes et matériaux divisés, CNRS UMR 7612, ESPCI, 10 rue Vauquelin, 75231 Paris, France, Laboratoire complexes macromoléculaires en cellules vivantes, Institut Jacques Monod, CNRS et Universités Paris 6 et 7, 4 place Jussieu, 75251 Paris, France, and Laboratoire d'optique physique, CNRS UPR5, ESPCI, 10 rue Vauquelin, 75231 Paris, France

Received December 3, 2004. In Final Form: February 14, 2005

Oils containing both fluorescent semiconductor and magnetic oxide nanoparticles are used to produce oil in water emulsions. This technique produces oil droplets with homogeneous fluorescence and high magnetic nanoparticle concentrations. The optical properties of the oil droplets are studied as a function of the droplet sizes for various concentrations of fluorescent and magnetic nanoparticles. For all concentrations tested, we find a linear variation of the droplet fluorescent intensity as a function of the droplet volume. For a given size and a given quantum dot (QD) concentration, the droplet fluorescence intensity drops sharply as a function of the magnetic nanoparticle concentration. We show that this decrease is due mainly to the strong absorption cross section of the magnetic nanoparticles and to a lesser extent to the dynamic and static quenching of the QD fluorescence. The role of the iron oxide nanoparticle localization in the droplet (surface versus volume) is also discussed.

Introduction

The production of beads or capsules in the micrometer size range that contain both magnetic iron oxide nanoparticles and fluorescent semiconductor quantum dots (QDs) has very recently started to be addressed.[1] Such materials have interesting potential applications since they combine the properties of purely magnetic micrometer-size beads that are used for a variety of biotechnology applications including cell sorting,[2,3] sensing,[4] and assay separations,[5] and the properties of purely fluorescent beads that are being developed as fluorescent labels for macromolecule detection[6] and multiplexed optical coding of biomolecules.[7]

QDs are colloidal, nanometer diameter, fluorescent semiconductor particles that have two main advantages compared to organic fluorophores: excellent photostability and an emission wavelength that is directly correlated (through quantum confinement) to their size. Consequently, beads of different colors can be obtained just by changing the size of the QD they contain.

The main limitation when it comes to designing beads (magnetic or not) containing QDs is that the QD emission spectrum is usually very sensitive to its environment: it can be partially or completely quenched because of free radicals[8] or inappropriate ligands.[9] After synthesis, QDs coated with hydrophobic ligands[9] are soluble in various kinds of organic nonpolar solvents such as alkanes, toluene, or chloroform. Attempts to transfer QDs in polar solvent, polymer matrixes, or water usually require adapted ligands and/or encapsulation of the QD in a protective shell.[10−12] Because of these characteristics, QD cannot be handled as easily as magnetic nanoparticles, and care needs to be taken to preserve the QD optical properties when producing QD-containing beads.

So far, QD-containing beads have been prepared using the doping of hydrophobic mesoporous materials (styrene or silica) with hydrophobic QDs.[7,13,14] These techniques preserve the QD optical properties, but dense nanoparticle filling (necessary to obtain strongly magnetic beads) has not yet been reported. QD-containing beads have also been prepared by QD encapsulation in silica[15] or styrene,[16] but these techniques often degrade the QD fluorescent properties.

The simultaneous encapsulation of both luminescent and magnetic oxide nanoparticles in polymer microcapsules has been demonstrated with water-soluble QDs and

* To whom correspondence may be addressed: benoit.dubertret@espci.fr.

[†] Laboratoire colloïdes et matériaux divisés, CNRS UMR 7612, ESPCI.

[‡] Laboratoire complexes macromoléulaires en cellules vivantes. Institut Jacques Monod, CNRS et Universités Paris 6 et 7.

[§] Laboratoire d'optique physique, CNRS UPR5, ESPCI.

(1) Gaponik, N.; Radtchenko, I. L.; Sukhorukov, G. B.; Rogach, A. L. *Langmuir* **2004**, *20*, 1449−1452.
(2) Levine, S. *Science* **1956**, *123*, 185−186.
(3) Melville, D.; Paul, F.; Roath, S. *Nature* **1975**, *255*, 706−706.
(4) Strick, T. R.; Allemand, J. F.; Bensimon, D.; Bensimon, A.; Croquette, V. *Science* **1996**, *271*, 1835−1837.
(5) Doyle, P. S.; Bibette, J.; Bancaud, A.; Viovy, J. L. *Science* **2002**, *295*, 2237−2237.
(6) Fein, M.; Unkeless, J.; Chuang, F. Y. S.; Sassaroli, M.; Dacosta, R.; Vaananen, H.; Eisinger, J. *J. Membr. Biol.* **1993**, *135*, 83−92.
(7) Han, M. Y.; Gao, X. H.; Su, J. Z.; Nie, S. *Nat. Biotechnol.* **2001**, *19*, 631−635.
(8) Sill, K.; Emrick, T. *Chem. Mater.* **2004**, *16*, 1240−1243.
(9) Murray, C. B.; Norris, D. J.; Bawendi, M. G. *J. Am. Chem. Soc.* **1993**, *115*, 8706−8715.
(10) Dubertret, B.; Skourides, P.; Norris, D. J.; Noireaux, V.; Brivanlou, A. H.; Libchaber, A. *Science* **2002**, *298*, 1759−1762.
(11) Wu, X. Y.; Liu, H. J.; Liu, J. Q.; Haley, K. N.; Treadway, J. A.; Larson, J. P.; Ge, N. F.; Peale, F.; Bruchez, M. P. *Nat. Biotechnol.* **2003**, *21*, 41−46.
(12) Gao, X. H.; Cui, Y. Y.; Levenson, R. M.; Chung, L. W. K.; Nie, S. M. *Nat. Biotechnol.* **2004**, *22*, 969−976.
(13) Gao, X. H.; Nie, S. M. *J. Phys. Chem. B* **2003**, *107*, 11575−11578.
(14) Stsiapura, V.; Sukhanova, A.; Artemyev, M.; Pluot, M.; Cohen, J. H. M.; Baranov, A. V.; Oleinikov, V.; Nabiev, I. *Anal. Biochem.* **2004**, *334*, 257−265.
(15) Rogach, A. L.; Nagesha, D.; Ostrander, J. W.; Giersig, M.; Kotov, N. A. *Chem. Mater.* **2000**, *12*, 2676−2685.
(16) O'Brien, P.; Cummins, S. S.; Darcy, D.; Dearden, A.; Masala, O.; Pickett, N. L.; Ryley, S.; Sutherland, A. J. *Chem. Commun.* **2003**, 2532−2533.

10.1021/la047025m CCC: $30.25
Published on Web 03/24/2005

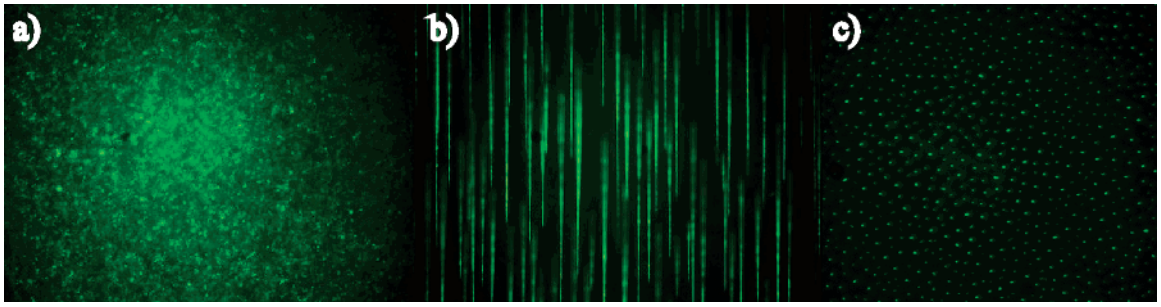

Figure 1. Fluorescent images of oil droplets containing $C_{max} = 51\%$ by weight iron oxide nanoparticles and 150 μM QD. The droplet average size is estimated at around few micrometers. (a) Without the magnetic field, the droplets have Brownian motion. Under the magnetic field, the droplets align parallel to the field lines within 2 s. In (b), the field lines are parallel to the cover slide surface; in (c) the field lines are perpendicular to the cover slide surface. The QD resistance to photobleaching is identical to that observed with QDs suspended in pure octane.

Fe_2O_3 magnetic nanoparticles. The drawback of this technique is that it uses QDs whose fluorescence does not last for more than 2 weeks in physiological buffer solutions.[1] Furthermore high iron oxide nanoparticle packing has not yet been demonstrated.

Most applications using magnetic beads benefit from high iron oxide particle concentration. When the beads are also fluorescent, this requirement, as we will see below, goes along with a strong decrease of the bead emission intensity.

Experimental Section

Ferrofluid composed of 70% weight α-Fe_2O_3 nanoparticles (around 10 nm diameter), 15% weight octane, and 15% weight oleic acid (OA) was purchased from Ademtech, France.

Core−shell 3 nm diameter CdSe/ZnS QDs were synthesized based on the methods introduced in Bawendi[9] and Guyot-Sionnest.[17] They emit with a maximum around 540 nm, have a size dispersion around 10%, and have a quantum yield of approximately 40%. They are coated with a mixture of tri-*n*-octylphosphine oxide and tri-*n*-octylphosphine.

A typical emulsion preparation is done as follows. Three milliliters of a 10 μM solution of QD is precipitated with an excess methanol. QDs are air-dried, suspended in 180 μL of octane, and then mixed with 0.45 g of ferrofluid (70% weight α-Fe_2O_3). This oil phase containing QDs and α-Fe_2O_3 nanoparticles is dispersed in a 6 wt % solution of nonyl phenol ethoxylate (NP-10, Sigma) in water up to a volume fraction of 60% to produce a pre-emulsion. The emulsion is obtained by shearing the solution using a mortar and a pestle. This crude emulsion can be stored for few days without any noticeable aging effect (droplet coalescence, ferrofluid leakage, or loss of fluorescence). The droplets are size-sorted using size-selective precipitation under a combination of magnetic and gravitational fields.[18] All droplet fluorescent images were performed with an inverted IX71 microscope (Olympus) with a 100× 1.34NA objective and recorded using a Pixelfly camera (PCO, Germany). Fluorescence intensity and individual droplet size were determined using ImageJ. Fluorescence spectra were recorded on a Fluoromax-2 (Jobin Yvon). Fluorescence lifetime images of the QD inside the droplets are obtained using a fluorescence decay microscope setup composed of a picosecond Ti−Sa laser with doubling and pulse picking (excitation 440 nm, 4 MHz) (Tsunami, Spectra Physics), a time- and space-correlated single photon counting detector (Europhoton GmbH, Germany), and an inverted microscope with a 100× 1.34NA oil objective (Leica).[19]

Results and Discussion

In this paper we present a simple method to produce droplets that are highly magnetic and fluorescent. We mix QDs with oleic acid stabilized iron oxide in a hydrophobic oil. As mentioned above, in hydrophobic oil, the QD stability, solubility, and optical properties are very good. This mixture is then fractionated into spherical droplets using standard emulsification techniques.[20] The concentration of magnetic and fluorescent particles in the droplets can be chosen precisely by tuning the amount of particles suspended in the hydrophobic oil. With this approach, fluorescent droplets with $C_{max} = 51\%$ in weight of iron oxide nanoparticles can be obtained. The droplet diameters range from a few hundred nanometers to a few tens of micrometers. Droplets can be sorted according to their size using size-selective precipitation (with a gravitational or a magnetic field).[18] The emulsion droplets are stable, and no aging effect is visible under the microscope. In principle, their surface could be further stabilized using ligand exchange and cross-linking techniques.[21] At high QD concentration (typically around 150 μM), the droplets appear as bright spheres under a fluorescent microscope. They are easily manipulated with a magnetic field. At high iron oxide particle concentration (c close to C_{max}), the droplets align within 2 s parallel to the field's line (Figure 1). The rapid droplet response to the magnetic field is in contrast with the 20 min necessary to align luminescent polymer microcapsules containing QD and iron oxide particles.[1] When the magnetic field is removed, the droplet alignment is immediately broken and the droplets disperse again within few seconds. The fluorescence inside the droplets appears very homogeneous as observed by fluorescence microscopy.

The main issue when encapsulating fluorescent nanoparticles with strongly absorbent iron oxide nanoparticles into micrometer size droplets is the influence of the mixing composition (ligands and nanoparticles concentration) on the QD emission intensity.

To address this problem we made emulsions with various nanoparticles and ligand concentrations. The iron oxide nanoparticle concentration ranged from 0 to $C_{max} = 51\%$ by weight, the QD concentration ranged from 150 to 450 μM, and the oleic acid concentration ranged from 0 to 8% in volume. For all nanoparticle concentrations and sizes (ranging between 0.5 and 5 μm in diameter) tested, we found that the droplet fluorescence intensity (I) varies linearly with the droplet volume and the QD concentration (C_{QD}) (parts a and b of Figure 2), i.e., $I = C_{QD} d^3 f(C_{ferro})$, where $f(C_{ferro})$ is a function of the iron oxide concentration, C_{ferro} is the concentration of ligands and surfactant in the system, and d is the droplet diameter.

(17) Hines, M. A.; GuyotSionnest, P. *J. Phys. Chem.* **1996**, *100*, 468−471.
(18) Bibette, J. *J. Magn. Magn. Mater.* **1993**, *122*, 37−41.
(19) Emiliani, V.; Sanvitto, D.; Tramier, M.; Piolot, T.; Petrasek, Z.; Kemnitz, K.; Durieux, C.; Coppey-Moisan, M. *Appl. Phys. Lett.* **2003**, *83*, 2471−2473.
(20) Mason, T. G.; Bibette, J. *Phys. Rev. Lett.* **1996**, *77*, 3481−3484.
(21) Wooley, K. L. *J. Polym. Sci. Polym. Chem.* **2000**, *38*, 1397−1407.

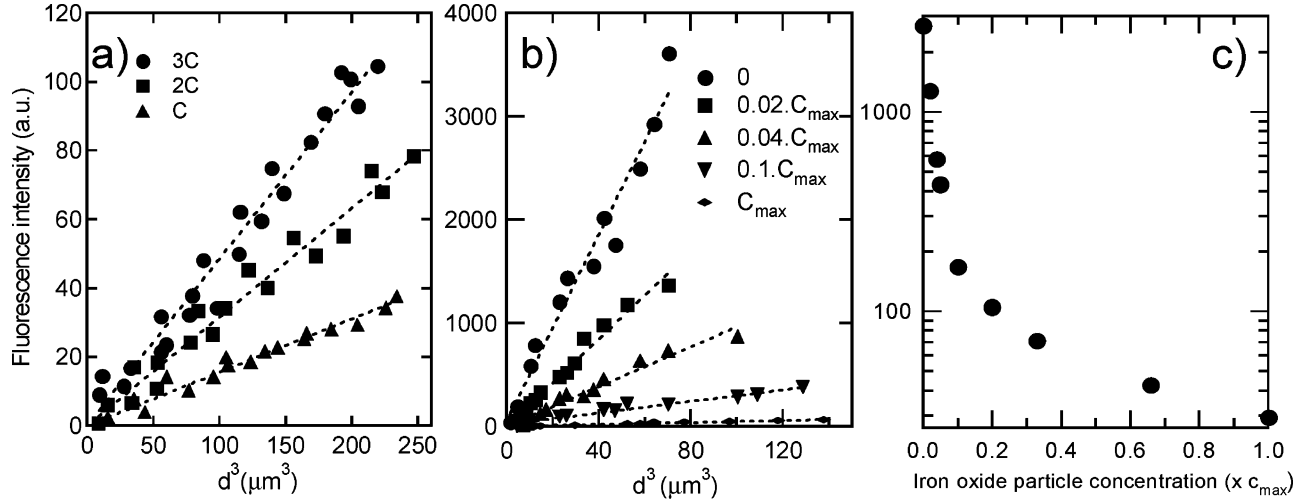

Figure 2. Fluorescence intensity variation of the oil droplets containing both iron oxide nanoparticles and QDs. (a) Fluorescence intensity evolution as a function of d^3 (d is the droplet diameter) of droplets containing 17% in volume ferrofluid and three different QD concentrations (C, $2C$, $3C$, with $C = 150$ μM). (b) Fluorescence intensity evolution as a function of d^3 of droplets containing $C = 150$ μM of QDs and five different ferrofluid concentrations (C_{max}, $0.1C_{max}$, $0.04C_{max}$, $0.02C_{max}$, $0C_{max}$, with $C_{max} = 51\%$ in weight). The iron oxide nanoparticle dilutions were carried out in pure octane. In (a) and (b), the dotted lines are the linear fits associated with each set of measurements. (c) Fluorescence intensity variation of $d = 3.7$ μm diameter droplets containing $C = 150$ μM QDs as a function of the ferrofluid concentration. $C_{max} = 51\%$ iron oxide nanoparticles in weight. The fluorescence intensity values reported are deduced from linear fits performed as in (b).

As shown in Figure 2b, the presence of iron oxide nanoparticles in the droplets strongly reduces their fluorescence intensity. However, for all ferrofluid concentrations tested the fluorescence intensity variation as a function of the droplet volume remains linear, suggesting that over the droplet size range explored (0.5−5 μm in diameter), the QDs partaking in the fluorescent signal scale as the droplet volume. A more detailed study of the influence of the ferrofluid concentration on the droplet fluorescence intensity is given in Figure 2c. The fluorescence intensity emitted by the droplets decreases by nearly 2 orders of magnitude when the iron oxide particle concentration varies from 0 to C_{max}. The decrease is very fast at low ferrofluid concentration. One order of magnitude in the fluorescent signal is lost when only 10% of the maximum iron oxide nanoparticle concentration is present in the droplets (Figure 2c).

This reduction could be due to the iron oxide nanoparticle absorption, to the QD's dynamic or static quenching, and/or to inhomogeneity in the iron oxide nanoparticle distribution inside the droplet. We tested each of these possibilities.

Both the light used to excite the QD (435 nm) and the light emitted by the QDs (with a maximum around 540 nm) are strongly absorbed by the α-Fe_2O_3 nanoparticles.[22] We computed[23,24] the absorption efficiency at 435 nm of droplets with a diameter ranging from 1 to 5 μm and ferrofluid concentration ranging from $C_{max}/10$ to C_{max}. The refractive index real part of the ferrofluid used for the experiments was chosen to be equal to 1.6.[22] Its imaginary part at 435 nm was measured to be $n_i = 0.05$ at 435 nm, for $C_{ferro} = C_{max}$. n_i was measured using the ferrofluid absorption at 435 nm for a set of diluted solutions.

We found that for all ferrofluid concentrations between $C_{max}/10$ and C_{max}, the absorption efficiency increases monotonically with the droplet diameter. Saturation (absorption efficiency of 1) is reached for 5 μm diameter droplets for $C_{ferro} = 0.6C_{max}$. At $C_{ferro} = C_{max}$, droplets with diameter > 2.2 μm have reached saturation. At saturation, all the light shone on the droplet is absorbed by the iron oxide nanoparticles and some QD are not excited at all. We also computed[24] the radial variation of the ratio of the internal/external absolute square excitation electric field $|E_i(r)|^2$ (for a unit amplitude incident field) and found that even for 5 μm diameter droplets with the highest concentration of iron oxide nanoparticles (the droplet with the highest absorption in our experiments), the ratio decreases monotonically from 0.3 for $r = 5$ μm to 0.1 for $r = 0$ (at the center of the sphere). This shows that even when the absorption efficiency is close to 1 (i.e., at saturation), in the range of sizes and iron oxide concentrations studied, the incident field depth penetration in the droplet is quite large compared to the droplet size. In this regime, deviations from a d^3 variation of the measured droplet fluorescence (expected at saturation) are not noticeable in our measurements.

The possibility of fluorescence quenching was explored using time-gated fluorescence detection on a fluorescence decay microscope setup.[19] For various ferrofluid concentrations, we measured the two-dimensional lifetime map of about six droplets. The average lifetimes for each droplet were very similar, and the lifetime distribution was very uniform over the droplet optical cut (Figure 3b,d) suggesting that no QD aggregation near the droplet surface or in the volume occurred. We found that the QD fluorescence lifetime decreased as the iron oxide concentration increased (Figure 3d,e). The QD emission intensity decreased by a factor of 4 because of dynamic quenching (most probably through dynamic quenching with the iron oxide nanoparticles) when the ferrofluid concentration is 1/3 of C_{max}. Larger iron oxide nanoparticle concentrations induce only slight increase in the quenching (Figure 3e).

QDs suspended in oleic acid (no octane) and emulsified in water as described above had similar average lifetime per droplet to an emulsion of QDs suspended in octane only (no oleic acid) (Figure 3f). We concluded that oleic acid did not induce any QD dynamic quenching. However, by using measurements in a fluorometer, we noticed that

(22) Ziolo, R. F.; Giannelis, E. P.; Weinstein, B. A.; Ohoro, M. P.; Ganguly, B. N.; Mehrotra, V.; Russell, M. W.; Huffman, D. R. *Science* **1992**, *257*, 219−223.

(23) Bohren C. F.; Huffman, D. R., *Absorption and Scattering of Light by Small Particles*; Wiley: New York, 1983.

(24) Matzler, C. MATLAB function for Mie scattering and absorption; Universitas Bernensis, 2002.

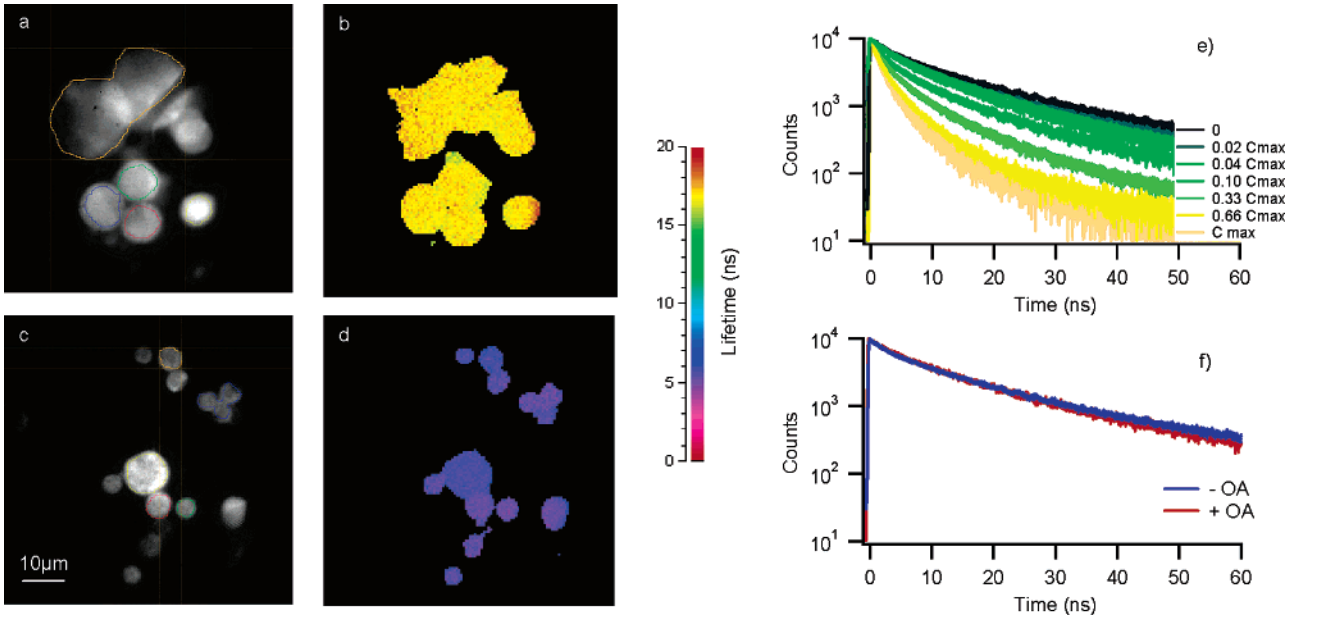

Figure 3. Fluorescence lifetime measurements on droplets containing $C = 150\ \mu$M QDs and different ferrofluid concentrations: (a) fluorescence intensity and (b) lifetime images of droplets containing only QDs; (c) and (d) of droplets containing $C = 150\ \mu$M QDs and $C_{max} = 51\%$ iron oxide nanoparticles in weight. The fluorescence decay of each droplet containing $C = 150\ \mu$M QDs and various ferrofluid concentrations (C_{max}, $0.66C_{max}$, $0.33C_{max}$, $0.1C_{max}$, $0.04C_{max}$, $0.02C_{max}$, 0) is measured, normalized, and plotted in (e). One sample was produced by emulsification of QDs in pure oleic acid, and its fluorescence decay was compared to an emulsion of QDs suspended in octane only (ferrofluid concentration = 0) in (f).

the QD fluorescence intensity decreases exponentially with the oleic acid volume fraction. An octane solution containing 8% in volume oleic acid has a fluorescence intensity that is three times less than when oleic acid is absent. The reason for this decrease is not known. Oleic acid has been used as a ligand for the QD synthesis.[25] Here QDs were synthesized with a TOP/TOPO mixture only, oleic acid was introduced after the synthesis. Since no dynamic fluorescence quenching was observed, we hypothesize that part of the QD population is completely quenched because of interactions of the oleic acid with the QD surface.

Last, we tested the effect of the homogeneity of the nanoparticle distribution on the droplet fluorescence intensity at low ferrofluid concentration. Indeed, changing the oleic acid concentration allows the tuning of the affinity of the oleic acid stabilized iron oxide nanoparticles for the droplet surface. This can be directly observed using a DIC setup for two oleic acid concentrations: at high OA concentration (8% in volume), the iron oxide is homogeneously distributed in the volume of the droplet, while at low OA concentration, the nanoparticles adsorb at the oil/water interface forming an iron oxide rich shell around an iron oxide poor solution in octane (Figure 4). We compared the droplet fluorescence intensity evolution as a function of the ferrofluid concentration when the ferrofluid is diluted in pure octane (Figure 2b,c) to that produced when the ferrofluid is diluted in octane solution containing 8% in volume oleic acid. We observed (data not shown) a slightly sharper fluorescent decrease when the ferrofluid is diluted in pure octane even after compensation for the oleic acid quenching effect. At low ferrofluid concentrations, if no oleic acid excess is present (Figure 2), the iron oxide nanoparticles localize on the droplet surface. This geometry produces a stronger fluorescence intensity decrease than when the droplets are filled homogeneously with the same amount of iron oxide.

(25) Yu, W. W.; Wang, Y. A.; Peng, X. G. *Chem. Mater.* **2003**, *15*, 4300−4308.

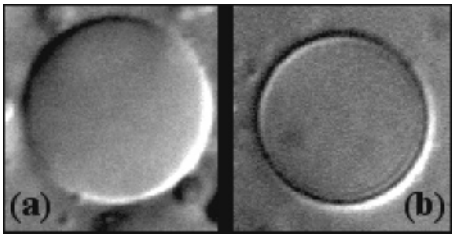

Figure 4. Differential interference contrast images of octane-in-water droplets stabilized by 6% by weight NP10. The inner phase contains 0.1% by volume iron oxide and oleic acid. At high OA volume fraction, 8% by volume (a), the inner phase is homogeneous; at low volume fraction, 0.1% by volume (b), iron oxide adsorbs at the droplet surface. The continuous phase refractive index was matched with that of the dispersed phase by addition of glycerol.

In conclusion, we report here a simple method to produce droplets containing both magnetic and fluorescent nanoparticles. This method is based on the emulsification in water of an oil containing oleic acid stabilized iron oxide particles and tri-*n*-octylphosphine stabilized QDs. While we show that we can obtain droplets that are fluorescent and strongly magnetic, we observe a decrease of the droplet fluorescence by a factor 100 when the iron oxide nanoparticle concentration ranges from 0 to 51% in weight (C_{max}). When the iron oxide concentration is close to C_{max}, we show that it decreases by a factor of 3 due to static fluorescence quenching and by a factor of 4 due to dynamic fluorescence quenching. We deduce that the iron oxide nanoparticles light absorption reduces the fluorescence emission by a factor of 8.3. At low ferrofluid concentration, we observed iron oxide nanoparticle localization at the droplet surface. This localization effect suggests that it may be possible, with a judicious choice of the nanoparticle ligands and the droplet surfactant, to localize the QDs at the droplet surface while the iron oxide particles are confined to an inner volume. Such geometry should enhance the droplet fluorescent emission.

Acknowledgment. M.T. acknowledges grants from FRM (ICP1.36), MRCT-CNRS, and ARC(4421). B.D. acknowledges grants from Le Ministère délégué à la recherche (ACI Jeunes chercheurs) and from La Société des Amis de l'ESPCI. B.D. thanks C. Boccara for very helpful discussions.

LA047025M